

Modern Physics Letters A
 © World Scientific Publishing Company

NEW BOUNDS ON THE STRING SCALE FROM FLAVOR PHYSICS

J. SANTIAGO

*IPPP, University of Durham,
 Durham, DH1 3LE, UK
 jose.santiago-perez@durham.ac.uk*

Received (Day Month Year)
 Revised (Day Month Year)

We review the very stringent lower bounds on the string scale that arise from flavor considerations in models with intersecting branes. Despite the absence of a realistic flavor structure at tree level, flavor changing interactions induce a non-trivial pattern of fermion masses and mixing angles when quantum corrections are taken into account. The resulting realistic theory of flavor allows us to constrain, in an unambiguous way, the string scale up to levels difficult to reconcile non-supersymmetric models.

Keywords: Intersecting branes; Flavor Changing Neutral Currents; Fermion Spectrum.

PACS Nos.: include PACS Nos.

1. Introduction

After the so-called second string revolution, string phenomenology has widen its subject beyond heterotic models. One very exciting possibility came across a few years ago through the realization that D-branes intersecting at non-trivial angles¹ allow for a neat way of breaking supersymmetry², generating four-dimensional chirality, and constructing in a bottom-up approach string models with a fully realistic matter and symmetry content³. A lot of effort has been put since in the study of the model building and phenomenology of such theories. (See⁴ for the initial works and⁵ for a more detailed introduction and references.) This intense dedication has resulted almost futile regarding the search of supersymmetric models. The restrictions from Ramond-Ramond tadpole cancellation are so strict that when added to the requirement of the preservation of $N = 1$ supersymmetry the resulting models are scarce and usually not fully realistic⁶, with extra exotic matter in the spectrum. (See however important progress in this direction in Ref.⁷.)

Given the fact that most of the realistic models presented so far are non-supersymmetric, a sensible question to ask is whether low scale non-fine-tuned models are phenomenologically allowed. A necessary previous step, to which we devote the first half for the present review, is the investigation of the structure of

flavor in these models. The trivial structure of tree level Yukawa couplings present in realistic models⁸ might seem discouraging at first sight. However the presence of flavor violating processes⁹, both at the string and field theory levels, propagates through quantum corrections to give a rich, realistic structure of fermion masses and mixing angles when one loop contributions are taken into account.

Armed with this realistic flavor structure we can study, in a quantitative unambiguous way, the phenomenological implications of low scale intersecting brane models. The same flavor violating four-point amplitudes that give raise to a realistic fermion spectrum induce important tree-level contributions to meson oscillations and rare processes. These are extremely well constrained experimentally, implying very stringent bounds on the string scale. (Incidentally, we should mention here that while tree level contributions to flavor violating processes decouple as the string scale increases, their contribution to the one loop Yukawa couplings does not.) In an attempt to be as comprehensive as possible and in order to minimize the possibility of fine-tuned situations in which the flavor violating contributions are small, we also discuss a new host of bounds on these models arising from flavor conserving amplitudes. Although the resulting constraints are much milder, still a lower bound on the string scale in the tens of TeV region is obtained.

2. Flavor Structure of Models with Intersecting Branes

Models with intersecting branes have a number of very interesting features such as the presence of chiral fermions, family replication and the possibility of constructing models with precisely the symmetries and the matter content of the Standard Model. Once a model has successfully passed such a coarse graining sift one has to more finely test it by for instance checking whether a realistic pattern of fermion masses and mixing angles can arise and what phenomenological predictions and restrictions it has. Two main ingredients enter the flavor structure of these models, one is the form of the Yukawa couplings, the other the presence of tree level flavor changing four point amplitudes. These two features are intimately related for, as we shall see, flavor violating operators are needed to generate a fully realistic pattern of fermion masses and mixings but at the same time, bounds on the string scale from the contribution of these operators to rare processes cannot be computed unless the flavor structure is known.

In order to make our arguments more specific, we shall concentrate on a particular model represented in Fig. 1⁸. It corresponds to an orientifold compactification of type II A theory with four stacks of D6-branes wrapping factorizable 3-cycles on the compact dimensions. The compactified space is a factorizable 6-Torus $T^2 \times T^2 \times T^2$, and the orientifold projection is given by $\Omega\mathcal{R}$ where Ω is the world-sheet parity and \mathcal{R} is a reflection about the horizontal axis of each of the three 2-tori,

$$\mathcal{R}Z_I = \bar{Z}_I.$$

We have denoted the coordinates of the tori by complex coordinates $Z_I = X_{2I+2} + iX_{2I+3}$, $I = 1, 2, 3$, so the three boxes in the figure represent each 2 torus, with

opposite edges being identified. The branes have four extended dimensions plus three compactified ones. Therefore, they appear as just lines in each T_2 . The net effect of the orientifold projection is to introduce mirror images of the branes in each T_2 (in the plane running horizontally).

The matter content of the low energy spectrum consists of massless chiral 4-dimensional fermions plus generally massive scalars, both living at branes intersections and transforming as bi-fundamentals of the corresponding gauge groups. The masses of the latter depend on the particular brane configuration (angle between branes) and can be considered as the superpartners of the fermions (for specific values of the angles in which they become massless, some $N = 1$ supersymmetry will be preserved by the corresponding intersection). Gauge bosons live in the world-volume of the branes, corresponding to unitary (orthogonal or symplectic groups are also possible for orientifold compactifications) gauge groups. Our particular model contains at low energies just the particle content and symmetries of the MSSM. In order to get that, the model contains four stacks of D6-branes, called *baryonic* (a), *left* (b), *right* (c), and *leptonic* (d). Three of the dimensions of each D6-brane wrap a 1-cycle on each of the three 2-tori, with wrapping numbers denoted by (n_k^I, m_k^I) , *i.e.* the stack k wraps n_k^I times the horizontal dimension of the I -th torus and m_k^I times the vertical direction. We have to include for consistency their orientifold images with $(n_k^I, -m_k^I)$ wrapping numbers. The number of branes in each stack, their wrapping numbers and the gauge groups they give rise to are shown in Table 1 and a subset of them, together with some of the relevant moduli, are displayed in Fig. 1.

Table 1. Number of branes, gauge groups and wrapping numbers for the different stacks in the model discussed in the text.

Stack	Name	N_k	Gauge group	wrapping numbers
a	<i>baryonic</i>	3	$SU(3) \times U(1)_a$	$(1,0);(1,3);(1,-3)$
b	<i>left</i>	1	$SU(2)$	$(0,1);(1,0);(0,-1)$
c	<i>right</i>	1	$U(1)_c$	$(0,1);(0,-1);(1,0)$
d	<i>leptonic</i>	1	$U(1)_d$	$(1,0);(1,3);(1,-3)$

A crucial feature that governs the whole flavor structure of these models is the fact that different families as well as the Higgs boson live at separate points in the compact dimensions. Yukawa interactions then correspond to instantonic contributions that are therefore expected to be proportional to the exponential of the relevant area connecting the three vertices. A more detailed study of Yukawa couplings, using calibrated geometry ⁸, and confirmed later by a proper string calculation using conformal field theory techniques ^{10,11}, showed that when the compact space is a factorizable torus and the branes wrap factorizable cycles, the relevant area is the sum of the *projected* areas of the triangle over each sub-torus.

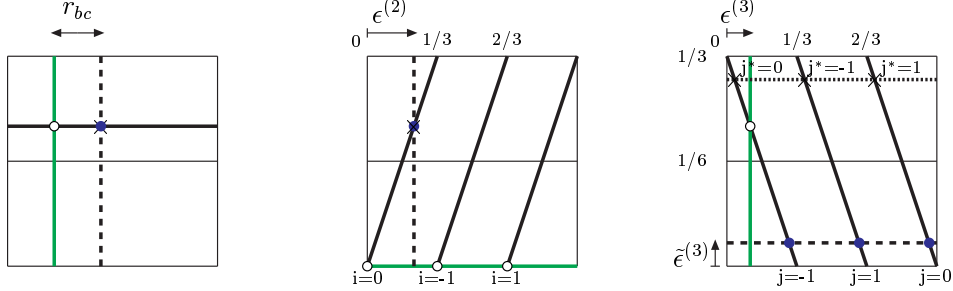


Fig. 1. Brane configuration in a model of D6-branes intersecting at angles. The leptonic sector is not represented while the baryonic, left, right and orientifold image of the right are respectively the dark solid, faint solid, dashed and dotted. The intersections corresponding to the quark doublets ($i = -1, 0, 1$), up type singlets ($j = -1, 0, 1$) and down type singlets ($j^* = -1, 0, 1$) are denoted by an empty circle, full circle and a cross, respectively. All distance parameters are measured in units of $2\pi R$ with R the corresponding radius (except $\tilde{\epsilon}^{(3)}$ which is measured in units of $6\pi R$)

The final result, including the quantum part reads

$$Y = \sqrt{2\lambda_{II}} 2\pi \sum_{I=1}^3 \sqrt{\frac{4\pi B(\nu_I, 1 - \nu_I)}{B(\nu_I, \theta_I) F(\nu_I, 1 - \nu_I - \theta_I)}} \sum_m e^{-\frac{A_I(m)}{2\pi\alpha'}}, \quad (1)$$

where we have neglected the presence of non-zero B field and Wilson lines and λ_{II} is the string coupling, B is the Euler Beta function, I runs over the three tori, ν_I and θ_I are the angles at the fermionic intersections, m runs over all possible triangles connecting the three vertices on each of the three tori (there is an infinite number of them due to the toroidal periodicity) and $A_I(m)$ is the projected area of the m -th triangle on the I -th torus.

Another important feature of the model is the fact that family *separation* occurs at a different torus for each chirality. As can be seen in Fig. 1, left handed fermions are split apart in the second torus (called hereafter *left* torus) whereas they are localized at the same point in the third torus (the *right* one). The opposite happens for the right handed fields. This fact, together with the previously mentioned that the couplings are proportional to the exponential of minus the *projected* areas, result in a trivial, factorizable form of the Yukawa couplings at tree level

$$(Y_u^{tree})_{ij} \sim a_i b_j^u, \quad (Y_d^{tree})_{ij} \sim a_i b_j^d. \quad (2)$$

The resulting spectrum is clearly unrealistic, with one massive and two massless generations. Nonetheless we will shortly see that the same feature of fermion splitting in the compact dimensions originates flavor violating four-point amplitudes that will contribute at loop level to give a non-trivial, fully realistic structure to the Yukawa couplings.

It has been known for long that models with split fermions suffer from flavor changing neutral current problems arising from the family non-universal couplings of the gauge boson KK modes¹². A detailed study of the four-point amplitudes¹¹

in these models uncovered new sources of flavor violation mediated by string instantons^{9,13}. These can be chirality preserving, whose contribution is again proportional to the exponential of the area of the corresponding quadrangle (with a non-zero area in only one torus for the leading contribution) or chirality changing, with a much richer structure and relevance regarding the generation of non-trivial one loop Yukawa couplings. It is the latter that we turn our attention to now.

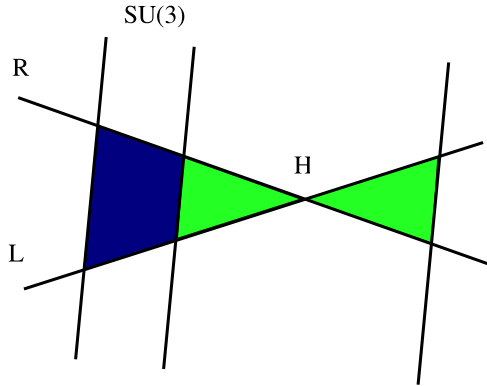


Fig. 2. Higgs-like processes mediated by the Higgs boson (green) and string instantons (blue). The former is proportional to the product of Yukawa couplings whereas the latter introduce new flavor structure.

We are interested in the following chirality changing four-point amplitudes (for concreteness we consider here quark fields as external particles)

$$\mathcal{A}_{ijkl}^{LR}(\bar{q}_{L_i} q_{R_j})(\bar{q}_{R_k} q_{L_l}).$$

At the field theory level, such amplitude can be originated by the exchange of the Higgs boson. This process is indeed reproduced in the string calculation, together with other processes, purely stringy in origin, that will be crucial to generate a non-trivial fermionic spectrum. For the sake of the discussion we concentrate for the moment on one particular sub-torus. The relevant amplitude corresponds to a four-sided polygon with two left handed and two right handed quarks as vertices. There are two possibilities for such a polygon, displayed in Fig. 2, one is obtained by adding together two triangular areas joined by the Higgs vertex (green area in the figure), the string calculation agrees with the intuition, giving a contribution proportional to the product of the two Yukawa couplings (one per triangle) and with a Higgs pole structure,

$$\mathcal{A}_{ijkl}^{LR} \sim \frac{Y_{ij} Y_{kl}^\dagger}{t - M_H^2}, \quad (3)$$

where we have shown the t -channel exchange for the sake of the example. The second possibility, represented in blue in the figure, lacks a field theory counterpart.

In the case that there is a non-zero area in just one torus, this contribution is again proportional to the exponential of the area swept out by the string connecting the four vertices, this time without running through a Higgs vertex and therefore being suppressed by the string scale instead of having a Higgs pole like the previous contribution. Two important effects are originated from this kind of diagrams, the first is already apparent now. Even in the case of non-zero area in just one torus, although the amplitude is factorizable, it is not proportional to the Yukawa couplings, therefore introducing new, yet too trivial to generate a fully realistic spectrum, flavor structure in the game. The second feature, this time enough to realize a realistic fermion spectrum happens when there are non-zero areas in more than one torus. In that case, as we shall see in a moment, factorization of the amplitude is lost and fully non-trivial new flavor structure is generated.

The technical reason for this non-factorization is the following. In order to perform the string calculation one maps the world-sheet into the upper complex plane, with the vertices in the real axis. Three of the vertices are conventionally fixed at positions 0, 1 and ∞ using $SL(2, R)$ invariance whereas one has to integrate over the position of the last one, that is situated at $0 < x < 1$. The classical contribution is then obtained by minimizing the action with respect to this parameter x and performing a saddle point approximation. The crucial point is that there is only *one* parameter x for *all* the three tori and although the minimization of the action for each torus gives the projected area in that torus, the value of x_{min} is usually not the same on the three of them and therefore the minimum of the total action does not correspond to the separate minimum of each sub-factor. Apart from the trivial cases in which the areas are equal up to rescaling in all tori or there is a non-zero area in just one torus, there are two (related) cases in which there is still factorization. One corresponds to three point amplitudes that give rise to Yukawa couplings, they are proportional to the projected areas and therefore factorize because we can fix the three vertices and there is not any extra free parameter that could make a difference between the different tori. The second case is chirality flipping amplitudes mediated by the Higgs field. In that case, the minimum of the action corresponds to $x_{min} = 1$, which is of course common to all tori.

We have seen that the tree level Yukawa couplings are factorizable and therefore too trivial for a realistic spectrum. Chirality and flavor changing amplitudes have been found of three different classes flavor wise, one is mediated by the Higgs boson, they are not only factorizable but also proportional to the tree level Yukawa couplings. The second class is that of factorizable but not proportional to Yukawa couplings contributions, these are for instance the ones in which there is a non-zero area in just one sub-torus. Finally there are other contributions that do not factorize, corresponding for instance to non-zero area of the blue type in Fig. 2 in more than one torus. The very rich structure present in four-point amplitudes propagates through quantum corrections to the Yukawa couplings. Even though a full string calculation is possible, we will treat threshold corrections at the field theory level, plugging the values of the chirality changing amplitudes we have just computed

as effective vertices. The one loop corrected Yukawa couplings have then a flavor dependence shown in Fig. 3. Corrections proportional to the Yukawa couplings give no new structure but just renormalizes the tree level values, factorizable but non proportional to Yukawa corrections increase the rank of the Yukawa matrix in one unit, therefore giving mass to the second generation. Finally, non-factorizable corrections give masses to all the three generations allowing therefore for a fully realistic spectrum. In fact, the different contributions we have just mentioned, give a rationale for the hierarchical spectrum observed in nature. Masses for the third family are generated at tree level, thus it is natural for them to be large. The first two generations, getting masses at one loop, are naturally much lighter than the third one. Furthermore, an extra hierarchy can naturally arise if the non-factorizable corrections are suppressed with respect to the factorizable ones. In order to test in a quantitative way our assertions, we have performed a fit to the quark masses and mixing angles reproducing reasonably well the observed spectrum and obtaining in this way a well defined flavor pattern that will allow us to give unambiguous predictions for the phenomenological implications of models with intersecting branes.

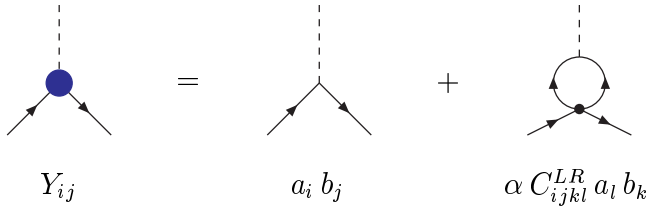


Fig. 3. Structure of Yukawa couplings including one loop threshold effects. The black dot corresponds to tree level chirality changing couplings.

The relevant (for flavor) parameters defining our model are, the horizontal and vertical ratios in the second and third torus, the position of the right brane in the second, $\epsilon^{(2)}$ and the third torus, $\tilde{\epsilon}^{(3)}$, the position of the left brane in the third torus, $\epsilon^{(3)}$, and the ratio of the up-type to down-type Higgs vevs ^a, $\tan \beta$. A reasonable value of the quark masses and mixing angles,

$$\begin{aligned} m_u &\sim 4 \times 10^{-3} \text{ GeV}, & m_c &\sim 1.8 \text{ GeV}, & m_t &\sim 176 \text{ GeV}, \\ m_d &\sim 4 \times 10^{-3} \text{ GeV}, & m_s &\sim 0.04 \text{ GeV}, & m_b &\sim 8 \text{ GeV}, \\ V_{12} &\sim 0.22, & V_{13} &\sim 0.003, & V_{23} &\sim 0.02, \end{aligned} \quad (4)$$

where we have included a global normalization factor 0.95 in the Yukawa couplings, is obtained for the following parameters (dimensional parameters are expressed in

^aAs we mentioned the low energy matter content is that of the MSSM, including two Higgs doublets.

string units)

$$\begin{aligned} R_1^{(2)} &= 1.1, & R_1^{(3)} &= 1.15, & \chi_2 &= 1.24, & \chi_3 &= 0.94, \\ \epsilon_2 &= 0.121, & \epsilon_3 &= 0.211, & \tilde{\epsilon}_3 &= 0.068, & \tan \beta &= 20. \end{aligned} \quad (5)$$

In this particular example, the full flavor structure is fixed, all the values of the relevant moduli, Yukawa couplings, rotation matrices, etc. are known in terms of the string scale. We can therefore compute without any ambiguity the values of any observable as a function of the string scale and obtain in that way precise bounds on it.

We would like to make one further remark before discussing the bounds on the string scale in these models. As we have said, the vast majority of the realistic models with intersecting branes presented in the literature so far are non-supersymmetric. It is to those that the specific mechanism for non-trivial fermion mass generation through Yukawa threshold effects apply. One should however consider the possibility of supersymmetric realistic models (as we will see in the next section the very constraining bounds on the string scale in these models makes it highly desirable for them to be supersymmetric) in which case non-renormalization theorems prevent threshold effects in Yukawa couplings. The very model we have presented possess a supersymmetric spectrum if the ratio of horizontal to vertical radii is equal in the second and third tori (hidden branes that break all the supersymmetries are anyway present in this model so even though the contribution we have computed would vanish in the “supersymmetric configuration”, there would be similar ones from strings stretching between the hidden and the MSSM sectors). Nevertheless, even in fully supersymmetric configurations, there are still sources of non-trivial flavor structure that can potentially lead to a realistic fermion spectrum. One possible source is for instance soft breaking A-terms. They have a different flavor structure than Yukawa couplings and this could be propagated through supersymmetric quantum loops to the Yukawa couplings. A detailed study of this and other effects is still necessary to see if realistic flavor patterns can be obtained as well in supersymmetric models.

3. Bounds on the String Scale

Once a realistic pattern of fermion masses and mixing angles has been developed we can compute, in a well-defined way, the effects of four-point string amplitudes in different observables in order to establish lower bounds on the string scale. The presence of flavor changing processes makes it more likely that rare processes are the most constraining ones. Nevertheless we will also consider the contribution to flavor conserving processes that give independent yet quite strict bounds on the string scale. We start our discussion with the former.

3.1. Flavor Violating Observables

Tree level flavor violating four-point amplitudes directly contribute to rare processes like meson oscillations and rare lepton and meson decays. These processes are loop

and sometimes GIM suppressed in the Standard Model and therefore very small. They are also extremely well constrained experimentally what makes of them a very powerful probe of flavor violating physics beyond the Standard Model. For this analysis, we have closely followed the discussion in Ref. 14, where the phenomenological implications of an extra $U(1)$ gauge boson with family non-universal couplings was considered. Of course, it has been extended to take into account not only the effects of gauge boson KK modes but also those of string instantons. Instead of giving a full account of the effect in each of the observables that have been considered, we will discuss in some detail the case of meson oscillations and refer to 14,13 for a more in-depth discussion.

The mass splitting for a meson with quark content $P_0 = \bar{q}_j q_i$, in the vacuum insertion approximation, reads,

$$\Delta m_P = \frac{2m_P F_P^2}{M_s^2} \left\{ \frac{1}{3} \text{Re} [A_{ijij}^{LL} + A_{ijij}^{RR}] - \left[\frac{1}{2} + \frac{1}{3} \left(\frac{m_P}{m_{q_i} + m_{q_j}} \right)^2 \right] \text{Re} A_{ijij}^{LR} \right\}, \quad (6)$$

where m_P and F_P are, respectively the mass and decay constant of the meson. Here A_{ijkl} are the dimensionless coefficients parameterizing the four fermion operators (with $1/M_s^2$ factored out).

Indirect CP violation in the Kaon system, which has been measured as well with extreme accuracy, is parametrized by

$$|\epsilon_K| = \frac{m_K F_K^2}{\sqrt{2} \Delta m_K M_s^2} \left\{ \frac{1}{3} \text{Im} [A_{dsds}^{LL} + A_{dsds}^{RR}] - \left[\frac{1}{2} + \frac{1}{3} \left(\frac{m_K}{m_d + m_s} \right)^2 \right] \text{Im} A_{dsds}^{LR} \right\}. \quad (7)$$

We compute the limits on the string scale requiring that the new contribution is smaller than the experimental value. This implies the following restrictions on the different coefficients,

- Kaon mass splitting

$$\frac{1}{M_s^2} |\text{Re} [A_{dsds}^{LL} + A_{dsds}^{RR}] - 17.1 \text{Re} [A_{dsds}^{LR}]| \lesssim 3.3 \times 10^{-7} \text{ TeV}^{-2}, \quad (8)$$

- B mass splitting

$$\frac{1}{M_S^2} |\text{Re} [A_{dbdb}^{LL} + A_{dbdb}^{RR}] - 3 \text{Re} [A_{dbdb}^{LR}]| \lesssim 2 \times 10^{-6} \text{ TeV}^{-2}, \quad (9)$$

- B_s mass splitting

$$\frac{1}{M_S^2} |\text{Re} [A_{sbsb}^{LL} + A_{sbsb}^{RR}] - 3 \text{Re} [A_{sbsb}^{LR}]| \lesssim 6.6 \times 10^{-5} \text{ TeV}^{-2}, \quad (10)$$

- D mass splitting

$$\frac{1}{M_S^2} |\text{Re} [A_{ucuc}^{LL} + A_{ucuc}^{RR}] - 3.9 \text{Re} [A_{ucuc}^{LR}]| \lesssim 3.3 \times 10^{-6} \text{ TeV}^{-2}, \quad (11)$$

- Kaon CP violation

$$\frac{1}{M_S^2} |\text{Im}[A_{dsds}^{LL} + A_{dsds}^{RR}] - 17.1 \text{Im}[A_{dsds}^{LR}]| \lesssim 2.6 \times 10^{-9} \text{ TeV}^{-2}. \quad (12)$$

It is clear that if the coefficients of the 4 fermion operators are order one (times $1/M_S^2$), the Kaon system puts a constraint $M_S \gtrsim 10^{3-4}$ TeV. Using the specific values of the rotation matrices found before we show in Table 2 that these estimations are indeed right.

The list observables is completed with $\mu - e$ coherent conversion in atoms, tau decays, and leptonic and semi-leptonic meson decays. Having developed a theory of fermion masses and mixing angles for the quark sector, we can only make an estimation of the bounds implied by these leptonic observables. Nevertheless, the order of magnitude of the bounds on the string scale implied by those is similar of the one found for quark observables, as shown in Table 2.

Table 2. Bounds on the string scale from flavor violating observables.

Quark Observables	M_s (TeV) \lesssim	(Semi)leptonic Observables	M_s (TeV) \lesssim
Δm_K	1400	$\mu - e$ conversion	1000
Δm_B	800	$\tau \rightarrow 3e$	2
Δm_{B_s}	450	$\tau \rightarrow 3\mu$	2
Δm_D	1100	$K_L^0 \rightarrow \mu^+ \mu^-$	260
$ \epsilon_K $	4×10^4	$K_L^0 \rightarrow \pi^0 \mu^+ \mu^-$	300

3.2. Flavor Preserving Observables

Flavor violating observables have proved extremely constraining in models with intersecting branes. The bounds obtained in the previous section should be considered as typical bounds for these models. The long list of observables we have studied makes it highly implausible that a choice of parameters (moduli) can be made for which *all* the flavor violating observables are strongly suppressed. In any case, in order to try and avoid that situation and for the sake of completeness we consider now the effects on flavor preserving observables. These effects rely more on very generic features of models with intersecting branes than in the particular structure of flavor. These features are, among others, the presence of several $U(1)$ gauge fields and the appearance of right handed neutrinos. For that reason we shall not use the detailed form of the rotation matrices to perform a very precise computation but will just estimate the effects and the corresponding bounds on the string scale.

We will start with a flavor conserving but CP violating observable, electric dipole moment (EDM) of (mainly mercury) atoms. EDM measurements mostly constrain operators of the type $\bar{d}_L d_R \bar{s}_R s_L$, $\bar{d}_L d_R \bar{b}_R b_L$, etc. Let us concentrate on the first

transition for definiteness. The relevant Lagrangian is therefore

$$\begin{aligned}\mathcal{L} &= \mathcal{A}_{ddss}^{LR} \bar{d}_L d_R \bar{\nu}_R \nu_L + \text{h.c.} \\ &= -\frac{1}{2} \text{Im} \mathcal{A}_{ddss}^{LR} (\bar{d} i \gamma_5 d \bar{s} s - \bar{s} i \gamma_5 s \bar{d} d) + \text{CP conserving part.}\end{aligned}\quad (13)$$

Using the recent analysis in Ref. 15 we can put the following bound on the corresponding coefficient,

$$\text{Im} \mathcal{A}_{ddss}^{LR} < 6 \times 10^{-11} \text{ GeV}^{-2}, \quad (14)$$

from the mercury EDM. The bounds on the other coefficients and the one coming from the neutron EDM are weaker than this one. Including typical values for the mixing angles we obtain the following (conservative) estimation for the bound on the string scale

$$M_s \gtrsim 10 \text{ TeV.} \quad (15)$$

The next effect we are going to consider is supernova cooling. For that we will use two rather generic features of models with intersecting branes, the presence of right handed neutrinos and the appearance of new $U(1)$ gauge groups that get masses (and therefore mix among themselves) through a generalized Green-Schwarz mechanism. The emission of right-handed neutrinos during supernova collapse can affect the rate of cooling. This implies the following constraint, for one species of light Dirac neutrinos,

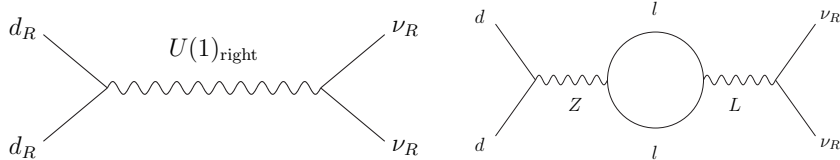
$$\Lambda \gtrsim 200 \text{ TeV}, \quad (16)$$

where Λ is the scale of the following quark-neutrino interaction

$$\mathcal{L}_R = \frac{4\pi}{\Lambda^2} \bar{q} \gamma_\mu \gamma_5 q \bar{\nu}_R \gamma^\mu \nu_R. \quad (17)$$

This effective interaction can be mediated by the “right” gauge boson (the one corresponding to the $U(1)$ gauge group in the right brane) at tree level as well as through the one loop mixing between the Z and the “leptonic” gauge bosons as represented in Fig. 4. The details of course depend on the particular values of the

Fig. 4. Tree (left) and one loop (right) level emission of right-handed neutrinos relevant for supernova cooling.



masses and couplings of the corresponding gauge bosons to the fermions. These were discussed in 16. A good estimation is however possible to make, taking into account

the different possibilities. We obtain the following (again conservative) bound from the tree level process

$$M_s \gtrsim 5 - 10 \text{ TeV}, \quad (18)$$

whereas the loop-suppressed process gives

$$M_s \gtrsim 1 \text{ TeV}. \quad (19)$$

Other processes like LEP constraints on contact interactions or the effects of the extra $U(1)$'s on the ρ parameter, lead to less stringent bounds on the string scale of the order of the TeV.

4. Conclusions

Models with intersecting branes have many phenomenologically appealing features. In order to further test their potential for fully realistic models, we have considered their flavor structure. In this way we have been able to compute in an unambiguous way their contributions to a number of flavor violating and preserving operators. The resulting bounds are very stringent

$$M_s \gtrsim 10^4 \text{ TeV}. \quad (20)$$

This feature will be generic in any string model in which the different generations of fermions live at separate points in the compact space. In that case, unless flavor violations are strongly suppressed (an example of this situation occurs in the warped case) for any reason, the high string scale implied by them is difficult to make compatible with a stabilized electroweak scale in non-supersymmetric models.

We should not be disappointed by these results. They should instead encourage us in the search of realistic supersymmetric models for which much higher string and compactification scales are stable against radiative corrections.

Acknowledgements

It is a great pleasure to thank S.A. Abel, O. Lebedev and M. Masip for collaboration and I. Navarro for useful discussions. This work has been funded by PPARC.

References

1. M. Berkooz, M. R. Douglas and R. G. Leigh, Nucl. Phys. B **480** (1996) 265 [arXiv:hep-th/9606139].
2. C. Bachas, arXiv:hep-th/9503030.
3. L. E. Ibañez, F. Marchesano and R. Rabadán, JHEP **0111** (2001) 002 [arXiv:hep-th/0105155].
4. R. Blumenhagen, L. Goerlich, B. Kors and D. Lust, JHEP **0010** (2000) 006 [arXiv:hep-th/0007024]; S. Forste, G. Honecker and R. Schreyer, Nucl. Phys. B **593** (2001) 127 [arXiv:hep-th/0008250]; G. Aldazabal, S. Franco, L. E. Ibañez, R. Rabadán and A. M. Uranga, JHEP **0102** (2001) 047 [arXiv:hep-ph/0011132]; G. Aldazabal, S. Franco, L. E. Ibañez, R. Rabadán and A. M. Uranga, J. Math. Phys. **42** (2001) 3103 [arXiv:hep-th/0011073].

5. S. Abel and J. Santiago, *J. Phys. G* **30** (2004) R83 [arXiv:hep-ph/0404237].
6. M. Cvetic, G. Shiu and A. M. Uranga, *Phys. Rev. Lett.* **87** (2001) 201801 [arXiv:hep-th/0107143]; M. Cvetic, G. Shiu and A. M. Uranga, *Nucl. Phys. B* **615** (2001) 3 [arXiv:hep-th/0107166]; D. Cremades, L. E. Ibañez and F. Marchesano, *JHEP* **0207** (2002) 009 [arXiv:hep-th/0201205]; R. Blumenhagen, L. Gorlich and T. Ott, *JHEP* **0301** (2003) 021 [arXiv:hep-th/0211059]; M. Cvetic, I. Papadimitriou and G. Shiu, arXiv:hep-th/0212177; M. Cvetic and I. Papadimitriou, *Phys. Rev. D* **67** (2003) 126006 [arXiv:hep-th/0303197]; M. Cvetic, P. Langacker and J. Wang, *Phys. Rev. D* **68** (2003) 046002 [arXiv:hep-th/0303208]; K. Behrndt and M. Cvetic, *Nucl. Phys. B* **676** (2004) 149 [arXiv:hep-th/0308045].
7. G. Honecker, *Nucl. Phys. B* **666** (2003) 175 [arXiv:hep-th/0303015].
8. D. Cremades, L. E. Ibañez and F. Marchesano, *JHEP* **0307** (2003) 038 [arXiv:hep-th/0302105].
9. S. A. Abel, M. Masip and J. Santiago, *JHEP* **0304** (2003) 057 [arXiv:hep-ph/0303087].
10. M. Cvetic and I. Papadimitriou, *Phys. Rev. D* **68** (2003) 046001 [arXiv:hep-th/0303083].
11. S. A. Abel and A. W. Owen, *Nucl. Phys. B* **663** (2003) 197 [arXiv:hep-th/0303124]; S. A. Abel and A. W. Owen, arXiv:hep-th/0310257.
12. A. Delgado, A. Pomarol and M. Quirós, *JHEP* **0001** (2000) 030 [arXiv:hep-ph/9911252]; C. D. Carone, *Phys. Rev. D* **61** (2000) 015008 [arXiv:hep-ph/9907362].
13. S. A. Abel, O. Lebedev and J. Santiago, arXiv:hep-ph/0312157.
14. P. Langacker and M. Plumacher, *Phys. Rev. D* **62** (2000) 013006 [arXiv:hep-ph/0001204].
15. D. Demir, O. Lebedev, K. A. Olive, M. Pospelov and A. Ritz, arXiv:hep-ph/0311314; O. Lebedev and M. Pospelov, *Phys. Rev. Lett.* **89** (2002) 101801 [arXiv:hep-ph/0204359].
16. D. M. Ghilencea, L. E. Ibanez, N. Irges and F. Quevedo, *JHEP* **0208**, 016 (2002); D. M. Ghilencea, *Nucl. Phys. B* **648**, 215 (2003).